Available online at www.eccomasproceedia.org
Eccomas Proceedia COMPDYN (2023) 2492-2504

ECCOMAS
Proceedia

COMPDYN 2023
9th ECCOMAS Thematic Conference on
Computational Methods in Structural Dynamics and Earthquake Engineering
M. Papadrakakis, M. Fragiadakis (eds.)
Athens, Greece, 12-14 June 2023

APPLICATION OF THE CONTINUOUS AIRY-BASED FOR STRESS SINGULARITIES (CASS) TO THE LOAD BEARING CAPACITY OF MASONRY STRUCTURES UNDER SEISMIC LOADS

Andrea Montanino[1], Francesca Linda Perelli[1], Daniela De Gregorio[1], and Giulio Zuccaro[1]

[1]Dept. of Structures for Engineering and Architecture, University of Naples Federico II
Via Claudio 21, 80125 Naples, ITALY
e-mail: {andrea.montanino, daniela.degregorio,zuccaro}@unina.it

Abstract. *The study of the behaviour of masonry structure is of large relevance for the preservation of architectural heritage, especially in areas subjected to seismic actions.*

This contribution provides a methodology for the evaluation of the maximum sustainable pseudo-static horizontal load, representative of a seismic action, under the framework of the Static Theorem of Limit Analysis. In particular, we adopt the Continuous Airy-based for Stress Singularities (CASS) method, consisting in the discretization of a domain in plate-type finite elements, for the identification of admissible stress fields in equilibrium with given external and internal loads, under the Heyman hypotheses of a normal, rigid, no tension material. In particular, the limit horizontal force is the maximum load for which an equilibrated solution still exists.

The considered application show the effectiveness of the method in dealing with the proposed problem, and is the base for the development of fragility curves for seismic curves at different local scales.

Keywords: Masonry buildings, No-tension materials, load bearing capacity, horizontal loads

ISSN:2623-3347
Peer-review under responsibility of the organizing committee of COMPDYN 2023.
doi: 10.7712/120123.10577.21347

1 INTRODUCTION

The large part of Italian and European architectural heritage is composed of masonry structures, in particular for what concerns religious buildings and historic residences. The preservation of this heritage is therefore of large interest for the scientific community, fostering the scientific research toward the development of simple, and at the same time, accurate models for the description of the behaviour of masonry materials. Indeed, masonry is a particular material, with an anisotropic behaviour, extremely rigid in compression, weakly reagent in traction, and with strong resistantce to sliding. For this reason, a large part of the most common commercial codes usually fail when dealing with masonry structures.

In recent years, masonry has been studied in different contexts (static or dynamic analyses, Limit Analysis), and adopting different modeling strategies (as a continuous medium, with block based discretisations, or macro-element discretisations). Each of them presents proper peculiarities and advantages.

Continuous methods allow to choice properly the discretisation method, regardless of the masonry constitution, block dimension, and other specific peculiarities. This category comprises Finite Element Method ([1, 2]), which need, however, complicated material models to deal with the material restrictions; on the other hand, its effectiveness in the description of the geometry of structures, even in the three dimensional case, makes this strategy particularly suitable when dealing with statics of large structure, under the effects of foundation settlements [3, 4]. Block based methods, on the contrary, are able to deal with the particular stereotomy of structures, describing precisely the block interlocking, and have a more clear understanding of the effects of the block dimensions. Among these methods, the Distinct Element Method [5, 6, 7] is widely adopted in sequential-static and dynamic analyses.

Limit-analyses based methods are often adopted to understand the level of safety of structures under different external actions. In this framework, the material model proposed by Heyman [8] of a Normal, Rigid, No-Tension (NRNT) material allows a strong simplification also for computational strategies. NRNT materials are characterised by an infinite resistance in compression, a vanishing strength in tension, and infinite resistance to sliding. All these condition are met in dry masonry structure when proper interlocking is assumed.

In the framework of the Limit-Analysis based methods, a classification can be made in displacement-based methods and force-based methods. In the first case, the Kinematic theorem is exploited, and the solution of the Boundary Value Problem is got through minimisation of a Total Potential Energy. Examples of this approach are the Piecewise Displacement Method (PRD) [9, 10, 11], the Continuous Displacement for Fractures (CDF) [12], and other rigid block models [13].

Force-based methods are commonly adopted for the assessment of the safety of vaults and domes, as in the case of the Thrust Network Analysis (TNA) [14, 15, 16, 17], based on the equilibrium of a network of forces as in a three-dimensional space frame structure. TNA has been extended to finite dimension blocks in [18]. A continuous version of the TNA is the Membrane Equilibrium Analysis (MEA), proposed in [19] and adopted to the equilibrium of several vaulted structures in [20, 21, 22, 23, 24]. An extension of MEA is provided in the shell-based methods [25, 26, 27, 28].

A large field of application of Limit-analysis based methods is the search for limit horizontal loads, representative, for example, of seismic actions. Both displacement- and force-based methods are applied in this case, as in [29, 30, 31].

In this paper, we propose an application of the Continuous Airy-based for Stress Singular-

ities (CASS) method [32] to the computation of the limit horizontal load that a 2D masonry structure, under the Heyman assumptions for NRNT material, can withstand. After recalling the mathematical formulation for NRNT material (Section 2) and the CASS-based discretisation (Section 3), the formulation is applied to the equilibrium of a square rigid block and to a masonry façade under body load and vertical distributed load, to compute the maximum seismic action that a typical masonry structure can resist.

2 MATERIAL MODEL

Let us consider a domain $\Omega \in \mathbb{R}^2$ made up of masonry material, under internal loads $\mathbf{b}$, defined in the interior of Ω, and contact loads $\mathbf{s}$, defined on the Neumann part of the domain, namely $\partial\Omega_N$. The remaining part of the domain boundary is the Dirichlet boundary $\partial\Omega_D$, on which displacements $\bar{\mathbf{u}}$ are assigned.

The equilibrium in the interior of the domain is given by

$$\nabla \cdot \mathbf{T} + \mathbf{b} = \mathbf{0}\,, \quad \mathbf{x} \in \Omega \quad , \tag{1}$$

where $\mathbf{T}$ is the stress tensor, $\nabla\cdot$ is the divergence operator, and $\mathbf{x}$ is the vector position in a three dimensional Cartesian reference frame. At the Neuman boundary, the equilibrium is imposed through

$$\mathbf{T}\mathbf{n} = \mathbf{s}\,, \quad \mathbf{x} \in \partial\Omega_N \quad , \tag{2}$$

being $\mathbf{n}$ the outward unit vector normal to the boundary, and $\mathbf{s}$ the given boundary traction.

The stress field must comply with the Heyman hypothesis of a no-tension material, that is, the material reacts only in compression. This conditions is expressed as

$$\mathbf{T} \in Sym^{-} \quad , \tag{3}$$

where Sym^{-} is the cone of symmetric, negative semidefinite tensors. This condition, in the 2D case, can be further expressed as

$$\mathrm{tr}\mathbf{T} \leq 0\,, \quad \mathrm{det}\mathbf{T} \geq 0 \quad . \tag{4}$$

The kinematic conditions on Ω are

$$\mathbf{E} = \frac{1}{2}\left(\nabla\mathbf{u} + \nabla\mathbf{u}^T\right)\,, \quad \mathbf{x} \in \Omega \quad , \tag{5}$$

where $\mathbf{E}$ the strain tensor, and $\mathbf{u}$ the displacement vector. In accordance with the Heyman material model, that is, only opening deformations are allowed, the strain tensor is positive semi-definite, which reads

$$\mathbf{E} \in Sym^{+} \quad . \tag{6}$$

At the Dirichlet boundary, the condition on assigned displacements holds, as

$$\mathbf{u} = \bar{\mathbf{u}}\,, \quad \mathbf{x} \in \partial\Omega_D \quad . \tag{7}$$

The Heyman normality condition is enforced as

$$\mathbf{T} \cdot \mathbf{E} = 0 \quad , \tag{8}$$

The global boundary value problem is therefore described by the following conditions

$$\begin{aligned} &div\mathbf{T} + \mathbf{b} = \mathbf{0} \quad , \quad \mathbf{T} \in Sym^{-} \quad , \quad \mathbf{Tn}\Big|_{\partial\Omega_N} = \mathbf{s} \quad , \\ &\mathbf{E} = \frac{1}{2}\left(\nabla\mathbf{u} + \nabla\mathbf{u}^T\right) \quad , \quad \mathbf{E} \in Sym^{+} \quad , \quad \mathbf{u}\Big|_{\partial\Omega_D} = \bar{\mathbf{u}} \quad , \\ &\mathbf{T}\cdot\mathbf{E} = 0 \quad . \end{aligned} \tag{9}$$

Such boundary value problem can be reformulated in terms of the minimisation of the Total Complementary Energy functional, giving raise to a force based formulation, or of a Total Potential Energy, leading to a displacement-based formulation.

In this work, we pursue the first strategy. The Total Complementary Energy for a rigid material is expressed as

$$E_c(\mathbf{T}) = -\int_{\partial\Omega_D} \mathbf{Tn}\cdot\bar{\mathbf{u}} ds \quad , \tag{10}$$

and the solution, in terms of stress field, is found through a suitable minimisation problem, formulated as

$$E_c(\mathbf{T}^0) = \min_{T\in\mathbb{H}} E_c(\mathbf{T}) \quad , \tag{11}$$

where $\mathbb{H}$ is the set of admissible stress fields, as defined in Equations (1)-(2)-(3), and reformulated as follows

$$\mathbb{H} = \left\{ \mathbf{T} \in \mathbb{R}^{2\times 2} \text{ s.t. } \nabla\cdot\mathbf{T} + \mathbf{b} = \mathbf{0}\,, \quad \mathbf{T}\in Sym^{-}\,, \quad \mathbf{Tn}\Big|_{\partial\Omega_N} = \mathbf{s} \right\} \tag{12}$$

2.1 Airy stress formulation

To reduce the number of unknowns and conditions of the present formulation, a convenient approach is the introduction of the scalar Airy stress potential F, defined as follows:

$$T_{11} = F_{,22}\ , \quad T_{22} = F_{,11} \quad T_{12} = -F_{,12} - (b_1 x_2 + b_2 x_1) \quad , \tag{13}$$

where x_1, x_2 are the directions of a Cartesian reference system, b_1, b_2 are the components of the internal load $\mathbf{b}$ on x_1, x_2, and the comma followed by an index, say i, indicates derivation with respect to the variable x_i.

The introduction of the Airy potential automatically satisfies the internal equilibrium; the boundary equilibrium, conversely, is satisfied by the introduction of suitable conditions on the the boundary values of the Airy stress function and on its normal slope, imposed as follows

$$F\Big|_{\partial\Omega_N} = m(s)\,, \quad \nabla F\cdot\mathbf{n}\Big|_{\partial\Omega_N} = n(s) \quad , \tag{14}$$

being $m(s)$ and $n(s)$ the contact bending moment and the contact axial force given by the load $\mathbf{s}$ on a frame structure shaped as the Neuman boundary of Ω [33].

Finally, the condition (3) on the negative semi-definiteness of the stress tensor is translated, following (13), into conditions on the Hessian of the Airy stress function, referred to as $\mathbf{H}(F)$, as

$$\mathrm{tr}\tilde{\mathbf{H}}(F) \le 0\,, \quad \det\tilde{\mathbf{H}}(F) \ge 0 \quad , \tag{15}$$

where $\tilde{\mathbf{H}}$ is a modified Hessian of the Airy stress potential, defined as

$$\tilde{\mathbf{H}}(F) = \begin{bmatrix} F_{,22} & -F_{,12} - (b_1 x_2 + b_1 x_2) \\ -F_{,12} - (b_1 x_2 + b_1 x_2) & F_{,11} \end{bmatrix} \quad . \tag{16}$$

Conditions (15) result into the requirement on the Airy stress potential of being concave within the domain Ω.

Summing up, the set $\mathbb{H}$ of the admissible stress tensor can be translated in the corresponding set of admissible stress potentials as

$$\begin{aligned}\mathbb{H}_F \quad = \Big\{ & F \in \mathbb{R} \text{ s.t.} \quad \mathrm{tr}\tilde{\mathbf{H}}(F) \leq 0\,, \quad \det\tilde{\mathbf{H}}(F) \geq 0\,, \\ & F\Big|_{\partial\Omega_N} = m(s)\,, \quad \nabla F \cdot \mathbf{n}\Big|_{\partial\Omega_N} = n(s) \Big\}\,.\end{aligned} \tag{17}$$

2.2 Limit load

Under the hypothesis of the Safe Theorem of the Limit Analysis, a masonry structure is safe when it exist at least one admissible stress field in equilibrium with internal and external loads, that is, the set $\mathbb{H}$ is not void.

Let us consider a varying contact load $\mathbf{s}$ as sum of a permanent load $\mathbf{s}_0$ and a varying contribution $\mathbf{s}_v$, as

$$\mathbf{s} = \mathbf{s}_0 + \lambda \mathbf{s}_v \tag{18}$$

where λ is a load multiplier i.e., proportional to the intensity of a seismic actions, following the traditional approach of pseudo-static loads for the evaluation of the load bearing capacity of structures under seismic actions.

Therefore, given Equation (18), the set of admissible stress fields, defined in (12), depends intrinsically on λ as follows:

$$\mathbb{H}^\lambda = \left\{ \mathbf{T} \in \mathbb{R}^{2\times 2} \text{ s.t. } \nabla \cdot \mathbf{T} + \mathbf{b} = \mathbf{0}\,, \quad \mathbf{T} \in Sym^-\,, \quad \mathbf{T}\mathbf{n}\Big|_{\partial\Omega_N} = \mathbf{s}_0 + \lambda \mathbf{s}_v \right\} \quad , \tag{19}$$

to which corresponds the set

$$\begin{aligned}\mathbb{H}_F^\lambda \quad = \Big\{ & F \in \mathbb{R} \text{ s.t. } \mathrm{tr}\tilde{\mathbf{H}}(F) \leq 0\,, \quad \det\tilde{\mathbf{H}}(F) \geq 0 \\ & F\Big|_{\partial\Omega_N} = m_0(s) + \lambda m^v(s)\,, \quad \nabla F \cdot \mathbf{n}\Big|_{\partial\Omega_N} = n_0(s) + \lambda n_v(s) \Big\}\,.\end{aligned} \tag{20}$$

where $n_0(s)$, $n_v(s)$, $m_0(s)$, and $m_v(s)$ are the counterparts of $m(s)$ and $n(s)$ for the permanent contact load $\mathbf{s}_0$ and the varying part $\mathbf{s}_v$.

The problem of the compatibility of given loads is reformulated as the search of the limit value of the load multiplier λ for which the set $\mathbb{H}$ (and therefore, $\mathbb{H}_F$) is non void. Assuming that the load $\mathbf{s}_0$ is compatible, that is

$$\mathbb{H}_F^0 \neq \emptyset \quad , \tag{21}$$

the search for the maximum varying load can be written as

$$\lambda_c = \max_{\mathbb{H}_F^\lambda \neq \emptyset} \lambda \quad , \tag{22}$$

where λ_c is the maximum admissible load multiplier, and $\lambda_c \mathbf{s}_v$ s the maximum variable load that the masonry structure can sustain, and therefore, can be regarded as a collapse load.

3 CONTINUOUS AIRY-BASED FOR STRESS SINGULARITIES

Problem (22) can be numerically solved through the Continuous Airy-based for Stress Singularities (CASS) method, a numerical discretisation method based on a plate-type finite element discretisation of the domain. A typical finite element adopted in the CASS method is shown in Figure 1, where i indicates the element node number, with $i = 1, ..., 4$, and $\hat{i}$, $i = 1, ...4$ are control points internal to the element.

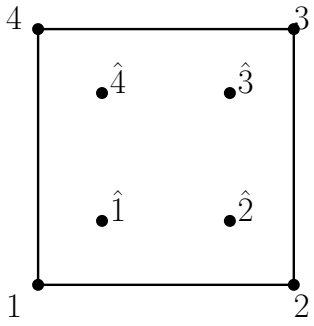

Figure 1: Standard finite element adopted in the CASS method

Each node of the discretisation is provided with three degrees of freedom, namely the value of the Airy stress potential, and of its derivatives in the x_1 and x_2 directions, that is

$$F^{el} = F^{el}(x_1, x_2; F^1, ..., F^4, F^1_{,1}, ..., F^4_{,1}, F^1_{,2}, ..., F^4_{,2}) \tag{23}$$

Therefore, the Airy stress function on each element is described by a twelve-term polynomial, as

$$F^{el} = \mathbf{c}(x_1, x_2)^T \mathbf{a} \tag{24}$$

being

$$\mathbf{c}^T = [1, x_1, x_2, x_1^2, x_1x_2, x_2^2, x_1^3, x_1^2x_2, x_1x_2^2, x_2^3, x_1^3x_2, x_1x_2^3], \quad \mathbf{a} = [a_1, ...a_{12}]^T \tag{25}$$

The coefficients $\mathbf{a}$ are retrieved through the imposition of the C^1-continuity conditions on the nodes of the discretisation. It is worth noting that, though the C^1-continuity is imposed on the nodes of the discretisation, this conditions is not extended to the whole element boundary, since the derivative in the normal direction to the boundary cannot be imposed with this discretisation. However, this is not a concern for the proposed approach, since the continuity of the derivative of the Airy stress potential in the normal directions implies continuity of the tangential component of the element boundary traction, which is not required by the boundary equilibrium.

Since the stress components are defined in terms of the second derivatives of the Airy stress potential, their continuity at the domain boundary cannot be enforced. The condition on the internal stress admissibility, that is the requirement of being negative semi-definite, can be imposed only in the interior of the domain. In particular we consider four internal points, to be placed in the interior of each element, as shown in Figure 1.

In particular, from Equations (24) and (25), it comes out that

$$\begin{aligned} \hat{T}_{11} \quad &= F^{el}{}_{,22} = \mathbf{c}^T_{,22}\, \mathbf{a} \\ \hat{T}_{22} \quad &= F^{el}{}_{,11} = \mathbf{c}^T_{,11}\, \mathbf{a} \\ \hat{T}_{12} \quad &= -F^{el}{}_{,12} - (b_1\hat{x}_2 + b_2\hat{x}_1) = -\mathbf{c}^T_{,12}\, \mathbf{a} - (b_1\hat{x}_2 + b_2\hat{x}_1) \quad . \end{aligned} \tag{26}$$

being $\hat{T}_{ij}$ the stress components in the control points.

By collecting Equations (26) for all the control nodes of the discretisation, the following linear relation can be formulated:

$$\begin{aligned} \hat{\mathbf{T}}_{11} &= \mathbf{K}_{11}\hat{\mathbf{F}} \\ \hat{\mathbf{T}}_{22} &= \mathbf{K}_{22}\hat{\mathbf{F}} \\ \hat{\mathbf{T}}_{12} &= \mathbf{K}_{12}\hat{\mathbf{F}} + \hat{\mathbf{b}} \quad . \end{aligned} \tag{27}$$

where $\hat{\mathbf{F}}$ is the array of nodal degrees of freedom, and $\hat{\mathbf{b}}$ collects the evaluation of the body load in the control points.

Therefore, the semi-definiteness of the stress tensor, in terms of the curvature of the Airy stress function, in discrete form, as

$$\begin{aligned} &(\mathbf{K}_{11} + \mathbf{K}_{22})\hat{\mathbf{F}} \leq 0 \\ &(\mathbf{K}_{11}\hat{\mathbf{F}}) \odot (\mathbf{K}_{22}\hat{\mathbf{F}}) - (\mathbf{K}_{12}\hat{\mathbf{F}} + \hat{\mathbf{b}}) \odot (\mathbf{K}_{12}\hat{\mathbf{F}} + \hat{\mathbf{b}}) \geq 0 \quad , \end{aligned} \tag{28}$$

where $\mathbf{C} = \mathbf{A} \odot \mathbf{B}$ is the Hadamard product between vectors $\mathbf{A}$ and $\mathbf{B}$, and is defined such that $C_i = A_i B_i$.

The boundary conditions involve directly the discretisation degrees of freedom, and can be written as

$$\mathbf{K}_{\partial\Omega_N}\hat{\mathbf{F}} = \hat{\mathbf{s}} \quad , \tag{29}$$

where $\hat{\mathbf{s}}$ is the array of the boundary conditions on the Airy stress function, following (14)

Introducing a discrete version of (18) into (29), we get

$$\mathbf{K}_{\partial\Omega_N}\hat{\mathbf{F}} = \hat{\mathbf{s}}_0 + \lambda\hat{\mathbf{s}}_v \quad , \tag{30}$$

leading to a final discrete version of the set $\mathbb{H}_F^\lambda$ as

$$\begin{aligned} \hat{\mathbb{H}}_F^\lambda = \Big\{ &\hat{\mathbf{F}} \in \mathbb{R}^N \text{ s.t. } (\mathbf{K}_{11} + \mathbf{K}_{22})\hat{\mathbf{F}} \leq 0\,, \\ &(\mathbf{K}_{11}\hat{\mathbf{F}}) \odot (\mathbf{K}_{22}\hat{\mathbf{F}}) - (\mathbf{K}_{12}\hat{\mathbf{F}} + \hat{\mathbf{b}}) \odot (\mathbf{K}_{12}\hat{\mathbf{F}} + \hat{\mathbf{b}}) \geq 0\,, \\ &\mathbf{K}_{\partial\Omega_N}\hat{\mathbf{F}} = \hat{\mathbf{s}}_0 + \lambda\hat{\mathbf{s}}_v \Big\}\,. \end{aligned} \tag{31}$$

The computation of the limit load (in terms of the collapse multiplier λ_c) is finally done through the maximisation of the load multiplier λ provided that the set of admissible, discrete stress potentials is non void, as

$$\lambda_c = \max_{\hat{\mathbb{H}}_F^\lambda \neq \emptyset} \lambda \quad . \tag{32}$$

4 APPLICATION

We apply the procedure proposed in previous Section to two different geometries: a panel under self-weight, and a uniform load on its top edge, and a masonry façade under self-weight and slabs load. For both problems, after describing the prescribed boundary conditions, we compute the solution in terms of collapse multiplier λ_c and show the corresponding principal stress field.

4.1 Rocking of a masonry square panel

We analyse the panel described in Figure 2, subjected to its self-weight $\mathbf{b} = 1$ N/m^3, a distributed vertical load on its top side $\mathbf{q} = 1$ N/m^2, and an horizontal force of intensity λP on the top left corner. The sample horizontal force is assumed as the sum of all vertical loads, and therefore, its value is $P = 2$ kN

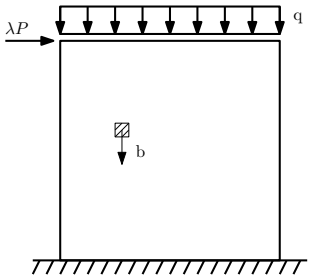

Figure 2: Geometry and loads on a square panel.

The boundary conditions associated to this load distribution are given in terms of the Airy stress potential as follows:

$$\begin{aligned}
&\text{left side:} && F = 0 && \nabla F \cdot \mathbf{n} = \frac{bL}{2} y \\
&\text{top side:} && F = -\frac{1}{8} q (L + 2x)^2 + \frac{1}{4} bHL(L + 2x) && \nabla F \cdot \mathbf{n} = -\lambda P + 1/8 by(L^2 - 4x^2) \\
&\text{right side:} && F = -\lambda P(H - y) + -q\frac{L^2}{2} + \frac{1}{2} bHL^2 && \nabla F \cdot \mathbf{n} = -Lq + b(HL - Ly/2)
\end{aligned} \tag{33}$$

Conditions (33) represent explicitly the boundary equilibrium in terms of the load multiplier λ. The solution of the problem in terms of load bearing capacity of the structure provides the maximum admissible load multiplier, also referred to as collapse multiplier.

The problem is discretised through the CASS method, and formulated in the discrete form (32). It solution provides a collapse load $\lambda = 0.33$ N, to which corresponds the principal stress distribution shown in Figure 3.

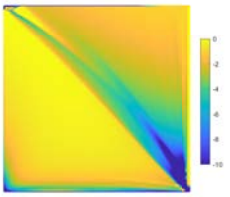

Figure 3: Minimum principal stress distribution in correspondence of the ultimate horizontal load

It is worth nothing that, contrariwise to the case of the absence of self-weight, where the load multiplier was $\lambda_c = 0.5$ (see [32]), in this case the maximum horizontal load is less than one third of the total vertical load.

4.2 A masonry façade under seismic load

In this section, CASS method is applied to the load bearing capacity of a two-story masonry façade under self-weight and slab loads.

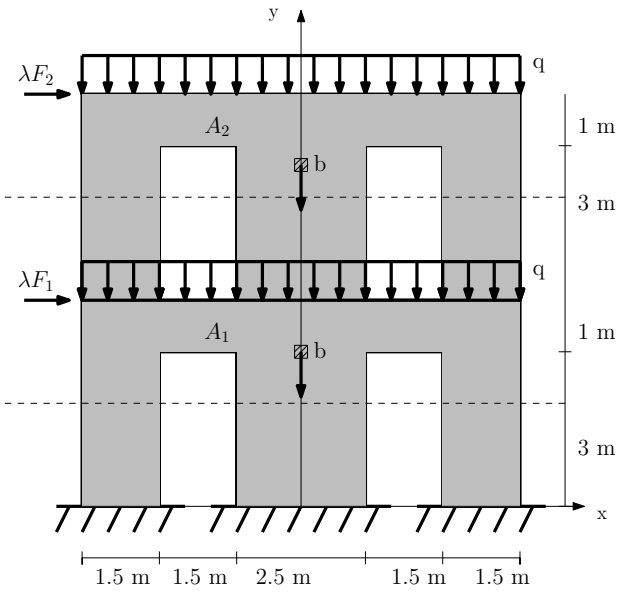

Figure 4: Geometry and loads of the masonry façade

The geometry and loads of the façade are depicted in Figure 4, where the distributed vertical load is $q = 25$ kN/m at both stories, and the vertical volume load is $b = 17.64$ kN/m^2.

The horizontal forces F_1 and F_2 are equal to the total vertical force affecting the areas A_1 and A_2, delimited by dashed lines in Figure 4. Considering both the self-weight and the slab loads, $F_1 = 600$ kN, and $F_2 = 460$ kN.

The CASS analysis returns a value of the load multiplier $\lambda = 0.30$, to which correspond the principal stress distribution shown in Figure 5.

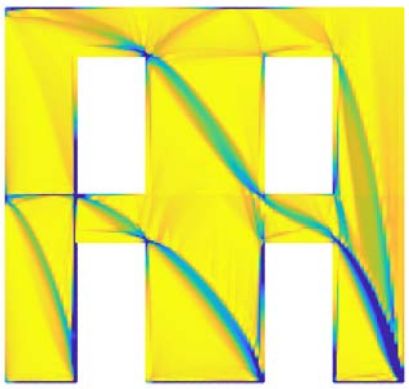

Figure 5: Minimum principal stress distribution corresponding to the limit horizontal load for the masonry façade.

From the analysis of Figure 5, it can be noted that the stress concentrate along small narrow bands that tart from the application points of the two horizontal loads and reach the opposite

corners. Actually, these stress bands represent preferential load paths for the structure, and develop as much as the limit load is approached. Such narrow bands are representative of singular stress fields, and their width is linked with the size of the discretisation.

The load multiplier can be translated into earthquake intensity, in terms of Peak Ground Acceleration (PGA) following the Italian standard NTC, as

$$PGA = \frac{\lambda_c q}{S} g \quad , \tag{34}$$

where λ_c is the collapse load multiplier, q is a ductility factor, set to 2, and S is the subsoil factor, fixed to 1.25. thus, for $\lambda_c = 0.3$, the corresponding Peak Ground Acceleration is $PGA = 0.48$ g.

5 CONCLUSIONS

In the present contribution we show the application of the CASS method to the analysis of the load bearing capacity of 2D masonry structures. In particular, after a brief discussion on the method, in the frame of NRNT material and the Static Theorems of Limit Analysis, the CASS discretisation has been shown, in the light of the problem of the search for a limit load. The CASS method has then been applied to the rocking of a square panel, under self-weight and a distributed load, and to a masonry façade, to compute the limit horizontal load on rigid slabs, and finally computing the theoretical maximum intensity of an earthquake, to which the masonry structure can resist.

The present approach can be adopted for the construction of force-based collapse curves, on the basis of the geometry and other constructive details of a large sample of buildings, from local to national scale, similarly to what has been done in [34] adopting a displacement-based approach.

REFERENCES

[1] Adrian W Page. Finite element model for masonry. *Journal of the Structural Division*, 104(8):1267–1285, 1978.

[2] AD Tzamtzis and PG Asteris. Finite element analysis of masonry structures: part i-review of previous work. In *North American Masonry Conference, Clemson, South Carolina*, 2003.

[3] Grigor Angjeliu, Giuliana Cardani, Dario Coronelli, et al. Digital modelling and analysis of masonry vaults. *International Archives of the Photogrammetry, Remote Sensing and Spatial Information Sciences*, 42:83–89, 2019.

[4] Grigor Angjeliu, Giuliana Cardani, and Dario Coronelli. A parametric model for ribbed masonry vaults. *Automation in Construction*, 105:102785, 2019.

[5] Dora Foti, Vitantonio Vacca, and Ivana Facchini. Dem modeling and experimental analysis of the static behavior of a dry-joints masonry cross vaults. *Construction and Building Materials*, 170:111–120, 2018.

[6] PB Laurenco, Jan G Rots, and Johan Blaauwendraad. Two approaches for the analysis of masonry structures: micro and macro-modeling. *HERON, 40 (4), 1995*, 1995.

[7] José V Lemos. Discrete element modeling of masonry structures. *International Journal of Architectural Heritage*, 1(2):190–213, 2007.

[8] Jacques Heyman. The stone skeleton. *International Journal of solids and structures*, 2(2):249–279, 1966.

[9] Antonino Iannuzzo, Tom Van Mele, and Philippe Block. Piecewise rigid displacement (prd) method: a limit analysis-based approach to detect mechanisms and internal forces through two dual energy criteria. *Mechanics Research Communications*, 107:103557, 2020.

[10] Antonino Iannuzzo, Alessandro Dell'Endice, Tom Van Mele, and Philippe Block. Numerical limit analysis-based modelling of masonry structures subjected to large displacements. *Computers & Structures*, 242:106372, 2021.

[11] Antonino Iannuzzo. Energy based fracture identification in masonry structures: The case study of the church of "pietà dei turchini". *Journal of Mechanics of Materials and Structures*, 14(5):683–702, 2019.

[12] Antonino Iannuzzo, Philippe Block, Maurizio Angelillo, and Antonio Gesualdo. A continuous energy-based numerical approach to predict fracture mechanisms in masonry structures: Cdf method. *Computers & Structures*, 257:106645, 2021.

[13] Francesco Portioli and Lucrezia Cascini. Assessment of masonry structures subjected to foundation settlements using rigid block limit analysis. *Engineering Structures*, 113:347–361, 2016.

[14] Philippe Block and John Ochsendorf. Thrust network analysis: a new methodology for three-dimensional equilibrium. *Journal of the International Association for shell and spatial structures*, 48(3):167–173, 2007.

[15] R Maia Avelino, Antonino Iannuzzo, Tom Van Mele, and Philippe Block. Assessing the safety of vaulted masonry structures using thrust network analysis. *Computers & Structures*, 257:106647, 2021.

[16] R Maia Avelino, Antonino Iannuzzo, Tom Van Mele, and Philippe Block. An energy-based strategy to find admissible thrust networks compatible with foundation settlements in masonry structures. *Mechanics Research Communications*, 125:103978, 2022.

[17] Francesco Marmo and Luciano Rosati. Reformulation and extension of the thrust network analysis. *Computers & Structures*, 182:104–118, 2017.

[18] Nicola A Nodargi and Paolo Bisegna. Generalized thrust network analysis for the safety assessment of vaulted masonry structures. *Engineering Structures*, 270:114878, 2022.

[19] Maurizio Angelillo and Antonio Fortunato. Equilibrium of masonry vaults. *Novel approaches in civil engineering*, pages 105–111, 2004.

[20] Andrea Montanino, Carlo Olivieri, Giulio Zuccaro, and Maurizio Angelillo. From stress to shape: Equilibrium of cloister and cross vaults. *Applied Sciences*, 11(9):3846, 2021.

[21] Concetta Cusano, Andrea Montanino, Carlo Olivieri, Vittorio Paris, and Claudia Cennamo. Graphical and analytical quantitative comparison in the domes assessment: The case of san francesco di paola. *Applied Sciences*, 11(8):3622, 2021.

[22] Carlo Olivieri, Maurizio Angelillo, Antonio Gesualdo, Antonino Iannuzzo, and Antonio Fortunato. Parametric design of purely compressed shells. *Mechanics of Materials*, 155:103782, 2021.

[23] Concetta Cusano, Andrea Montanino, Claudia Cennamo, Giulio Zuccaro, and Maurizio Angelillo. Geometry and stability of a double-shell dome in four building phases: the case study of santa maria alla sanità in naples. *International Journal of Architectural Heritage*, pages 1–27, 2021.

[24] Concetta Cusano, Grigor Angjeliu, Andrea Montanino, Giulio Zuccaro, and Claudia Cennamo. Considerations about the static response of masonry domes: A comparison between limit analysis and finite element method. *International Journal of Masonry Research and Innovation*, 6(4):502–528, 2021.

[25] NA Nodargi and P Bisegna. A new computational framework for the minimum thrust analysis of axisymmetric masonry domes. *Engineering Structures*, 234:111962, 2021.

[26] NA Nodargi and P Bisegna. Minimum thrust and minimum thickness of spherical masonry domes: A semi-analytical approach. *European Journal of Mechanics-A/Solids*, 87:104222, 2021.

[27] Francesco Barsi, Riccardo Barsotti, and Stefano Bennati. Studying the equilibrium of oval-base pointed masonry domes: the case of pisa cathedral. *International Journal of Masonry Research and Innovation*, 7(1-2):146–171, 2022.

[28] F Barsi, R Barsotti, and S Bennati. Admissible shell internal forces and safety assessment of masonry domes. *International Journal of Solids and Structures*, page 112082, 2022.

[29] Antonio Fortunato, Fernando Fraternali, and Maurizio Angelillo. Structural capacity of masonry walls under horizontal loads. *Ingegneria Sismica*, 31(1):41–49, 2014.

[30] Antonino Iannuzzo, Carlo Olivieri, and Antonio Fortunato. Displacement capacity of masonry structures under horizontal actions via prd method. *Journal of Mechanics of Materials and Structures*, 14(5):703–718, 2019.

[31] Nicola A Nodargi and Paolo Bisegna. A finite difference method for the static limit analysis of masonry domes under seismic loads. *Meccanica*, 57(1):121–141, 2022.

[32] Andrea Montanino, Daniela De Gregorio, Carlo Olivieri, and Antonino Iannuzzo. The continuous airy-based for stress-singularities (cass) method: an energy-based numerical formulation for unilateral materials. *International Journal of Solids and Structures*, 256:111954, 2022.

[33] M Angelillo, A Fortunato, A Montanino, and M Lippiello. Singular stress fields in masonry structures: Derand was right. *Meccanica*, 49:1243–1262, 2014.

[34] Francesca L Perelli, Daniela De Gregorio, Andrea Montanino, Carlo Olivieri, and Giuseppe Maddaloni. Energy-based modelling of in-plane fragility curves for the 2d ultimate capacity of italian masonry buildings. *Frontiers in Built Environment*, 2023.